A new class of control structures for heterogeneous reactive distillation processes

Moraru, Mihai Daniel; Patrascu, Iulian; Kiss, Anton A.; Bildea, Costin Sorin

DOI
10.1016/j.cep.2021.108672

Publication date
2022

Document Version
Final published version

Published in
Chemical Engineering and Processing - Process Intensification

Chemical Engineering & Processing: Process Intensification 171 (2022) 108672

Contents lists available at ScienceDirect

Chemical Engineering and Processing - Process Intensification

journal homepage: www.elsevier.com/locate/cep

A new class of control structures for heterogeneous reactive distillation processes

Mihai Daniel Moraru [a], Iulian Patrascu [b], Anton A. Kiss [c,d], Costin Sorin Bildea [b,*]

[a] Hexion, Department of Technology, Engineering and Projects, Seattleweg 17, 3195 ND Pernis, the Netherlands
[b] University "Politehnica" of Bucharest, Polizu 1-7, 011061 Bucharest, Romania
[c] Department of Chemical Engineering and Analytical Science, The University of Manchester, Sackville Street, Manchester, M13 9PL, United Kingdom
[d] Department of Chemical Engineering, Delft University of Technology, Van der Maasweg 9, 2629 HZ, Delft, the Netherlands

ARTICLE INFO

Keywords:
Process control
Reactive distillation
Case studies
Esterification

ABSTRACT

There are only a handful of process control structures applied to the neat operation of both homogeneous and heterogeneous reactive distillation, for two-reactants / two-products one-reaction systems. All of these control structures employ inferential temperature control (or concentration analyzers) at some location in the column to balance the reaction stoichiometry.

This original study proposes a new class of control structures applicable to heterogeneous reactive distillation. The novel idea, common to all control structures, is based on monitoring the inventory of the reactant involved in the heterogeneous azeotrope. The organic reflux (or the organic reflux / aqueous distillate ratio) is used to detect the excess or deficiency of the reactant, based on which the fresh feed rate is adjusted such that the reaction stoichiometry is balanced. This control philosophy is simple and easy to implement in different ways as illustrated by several case studies. The performance of the proposed control structures depends on the system studied. For some systems, the performance is better, as good or nearly as good as that of the literature control structures. But for other systems, the performance is poor or the structure even fails to control the process, due to the insufficient feedback from inventory measurements.

1. Introduction

Reactive distillation (RD) is one of the best success stories of industrially implemented process intensification techniques, which offers major advantages such as reduced capital and operating costs [1]. However, the controllability of the intensified process is just as important as the economics since the required plant capacity, products purity and reaction stoichiometry must be achieved.

Invited for the Special Issue "*From distillation to hybrid and reactive separations – A tribute to Andrzej Górak*", the aim of this paper is to bring novel elements regarding the control of heterogeneous reactive distillation applied to esterification processes of industrial importance involving a two-reactant, one-reaction system. This paper proposes a new class of control structures that uses information regarding the decanter organic phase to feed the fresh reactants such that the reaction stoichiometry is fulfilled. The main idea, having its roots in the plant-wide control concepts [2,3], is that the level of the organic phase in the decanter is an indication of the inventory of the reactant involved in a heterogeneous azeotrope. As this level is conventionally controlled by the reflux rate, an increase / decrease of the reflux (or, equivalently, of the reflux ratio) is a warning that the reactant is accumulating / depleting, therefore its fresh feed rate must be adjusted. Thus, variables which are easy to measure (besides temperatures on some stages, as used in literature control structures) are available for implementing feedback loops which ensure that the reactants are fed in the correct ratio.

Among the reaction systems that can be efficiently carried out by reactive distillation, an important class is quaternary systems comprising of two reactants and two products. Rather often, one product is the high-boiling species (ester) that is obtained as bottom stream, while the other product (water) forms a low-boiling heterogeneous azeotrope (with the alcohol) that is obtained as distillate and further separated by exploiting a liquid-liquid split in a decanter. The reactant-rich (organic) phase is returned to the column as reflux, while the product-rich (aqueous) phase allows obtaining the top-product with a relatively high-purity. This process setup is known as heterogeneous reactive distillation [4] and is encountered in numerous chemical

* Corresponding author.
E-mail address: sorin.bildea@upb.ro (C.S. Bildea).

https://doi.org/10.1016/j.cep.2021.108672
Received 16 March 2021; Received in revised form 27 September 2021; Accepted 11 October 2021
Available online 16 October 2021

processes in which various acids are reacted with higher alcohols to produce esters. Esterification is an example of much industrial relevance, including the production of n-propyl propionate [5], n-butyl acrylate [6], 2-ethylhexyl acrylate [7], triacetin [8], fatty acid esters [9, 10], to name just a few.

Compared to conventional reaction-separation-recycle systems, the integration of reaction and separation in a single unit such as RD is perceived as a source of control problems that must be addressed, sometimes already at the design stage [11,12,13,14,15]. As RD is a very non-linear process, advanced process control strategies have been proposed, based on model predictive control for example [16,17].

In case of neat operation of RD, the reactants are fed in the stoichiometric ratio. This allows obtaining the bottom and distillate products with high purities, avoiding thus the need of an additional column to separate one product from the excess reactant. Common control objectives are related to setting the desired production rate, keeping the product purities at the required values and maintaining the component inventory (or differently said, balancing the reaction stoichiometry). Usually, the production rate is set by one of the fresh reactants, and sometimes, by the reboiler duty. In the case of homogeneous reactive distillation, the purity of the top product is usually achieved as for conventional distillation. In the particular case of heterogeneous RD, both decanter-outlet flows are always used for controlling the level of organic and aqueous phases. Therefore, one degree of freedom (such as reflux rate, distillate rate, or reflux/distillate ratio) is no longer available. Finally, the need of balancing the stoichiometry of the reaction makes the control more difficult [18], as it cannot be achieved by simple ratio or other feed-forward control scheme, due to unavoidable measurement and control implementation errors [19]. Note that, from the plantwide control point of view, heterogeneous reactive distillation is a two-reactant, one-reaction system [2]. In this case, only one reactant can have its feed flow rate fixed - and its inventory would be self-regulating, but a feedback mechanism is necessary to avoid accumulation / depletion of the second reactant [2,3]. Moreover, control structures that employ only inferential temperature control are preferred over concentration control schemes, because concentration control requires analyzers for composition measurement. In general, these analyzers are slow, expensive and require maintenance. Therefore, simple, robust, and inexpensive inferential control is desired to balance the reaction stoichiometry in neat operation of RD columns.

This paper is organized as follows. The next section presents and discusses both the control structures found in the literature and those proposed in this work; the new idea is introduced and described by means of three possible implementations. Then, the new control structures are tested and compared to the literature ones by means of five case studies of increasing complexity, covering a wide range of thermodynamic features. The paper ends with conclusions and some recommendations.

2. Control of reactive distillation

The literature review detailed in the next sub-sections shows that there is no standard control structure applicable to all RD systems involving two reactants, but in fact there are several structures which try to solve in different ways the problem of feeding the reactants in the right ratio, complying with the reaction stoichiometry. These structures are then evaluated by dynamic simulation and the best one is chosen for implementation.

The chemical system, on which all control structures are tested, involves a heavy reactant (acid or alcohol) fed in the column above the feeding location of a light reactant (acid or alcohol). The alcohol and the light product (water) form a low boiling heterogeneous azeotrope which is subject to phase separation in the decanter.

2.1. Literature control structures

Fig. 1 (left column) presents three different control structures, suggested in the literature, which attempt to fulfil, in different ways, the main control objectives of reactive distillation: production rate, product purity and reaction stoichiometry. Note that these control structures apply to both, homogeneous and heterogeneous reactive distillation systems.

Control structure S-1 [20] uses the reboiler duty (or vapour boilup) to set the production rate. The flow rates of both fresh reactants are used (directly or involving ratio control as shown in Fig. 1) to keep two temperatures in the column at constant values. These two control loops work together to achieve the specified product purity and to feed the reactants in the correct stoichiometric ratio. Luyben and Yu [13] apply this control structure to several processes for acetic acid esterification. They point out that selection of the trays on which to control temperature is the main issue in S-1, recommending that the trays should be selected such that the steady state gain between flow rate and temperature is negative.

Control structure S-2 [4] fixes the flow rate of one reactant (throughput manipulator) and uses the flow rate of the second reactant (directly or involving ratio control as shown in Fig. 1) and the reboiler duty to control two temperatures in the column. This was applied for RD processes for obtaining butyl propionate and butyl acetate [4], the temperature-controlled trays being identified by non-square relative gain array analysis. Control structures based on the same idea were also applied for RD processes for production of amyl acetate [21], triacetin [8], butyl and amyl acetates [22], n-propyl propionate [5], butyl levulinate [23], dimethyl carbonate [24], 1,3-dioxolane [25], various esters of acetic acid [13], diphenyl carbonate [26]

The differences between control strategies underlying S-1 and S-2 were analysed by Kaymak and Luyben [18], for an ideal reaction system and for methyl acetate process. The authors concluded that the selection of the manipulated fresh feed stream in S-2 has an important role in the stability of the system. Although S-2 is the most popular in the literature, one should also note one unusual feature – namely the use of reboiler duty to control one temperature on an upper stage, most of the time located in the upper part of the reactive section, while the flow rate of the heavy reactant (fed on the upper part of the reactive section) is used to control a temperature in the lower part of the column (one tray from the stripping section).

Control structures similar to S-3 were applied for the RD processes for butyl acrylate [27] and butyl levulinate [23]. S-3 uses the flow rate of one fresh reactant to set the production rate. The ratio between the reboiler duty and the flow rate of the limiting reactant is kept constant. The second fresh reactant (or the reactants ratio, as shown in Fig. 1) is used to control one temperature in the column. It is worth mentioning that the same authors [27] investigated another control structure which fixed the ratio between fresh reactants. As expected, this strategy failed for the case of unmeasured disturbances, such as contamination with water of one reactant.

2.2. A new class of control structures for heterogeneous reactive distillation

Fig. 1 (right column) illustrates three new control structures [28] which can be applied to heterogeneous reactive distillation (note that these structures do not apply to homogeneous reactive distillation). The applicability of these structures to heterogeneous reactive distillation can be analysed based on key thermodynamic data, namely, boiling points, azeotropy and liquid-liquid equilibria [29].

In all control structures, the light reactant sets the production rate. The quality of the bottom product is controlled by the reboiler duty. The feedback necessary to set the correct ratio between fresh reactants is obtained from the measured reflux ratio (S-4) or reflux rate (S-5). In S-6, a part of the alcohol is fed in the decanter. The reflux ratio (or the reflux

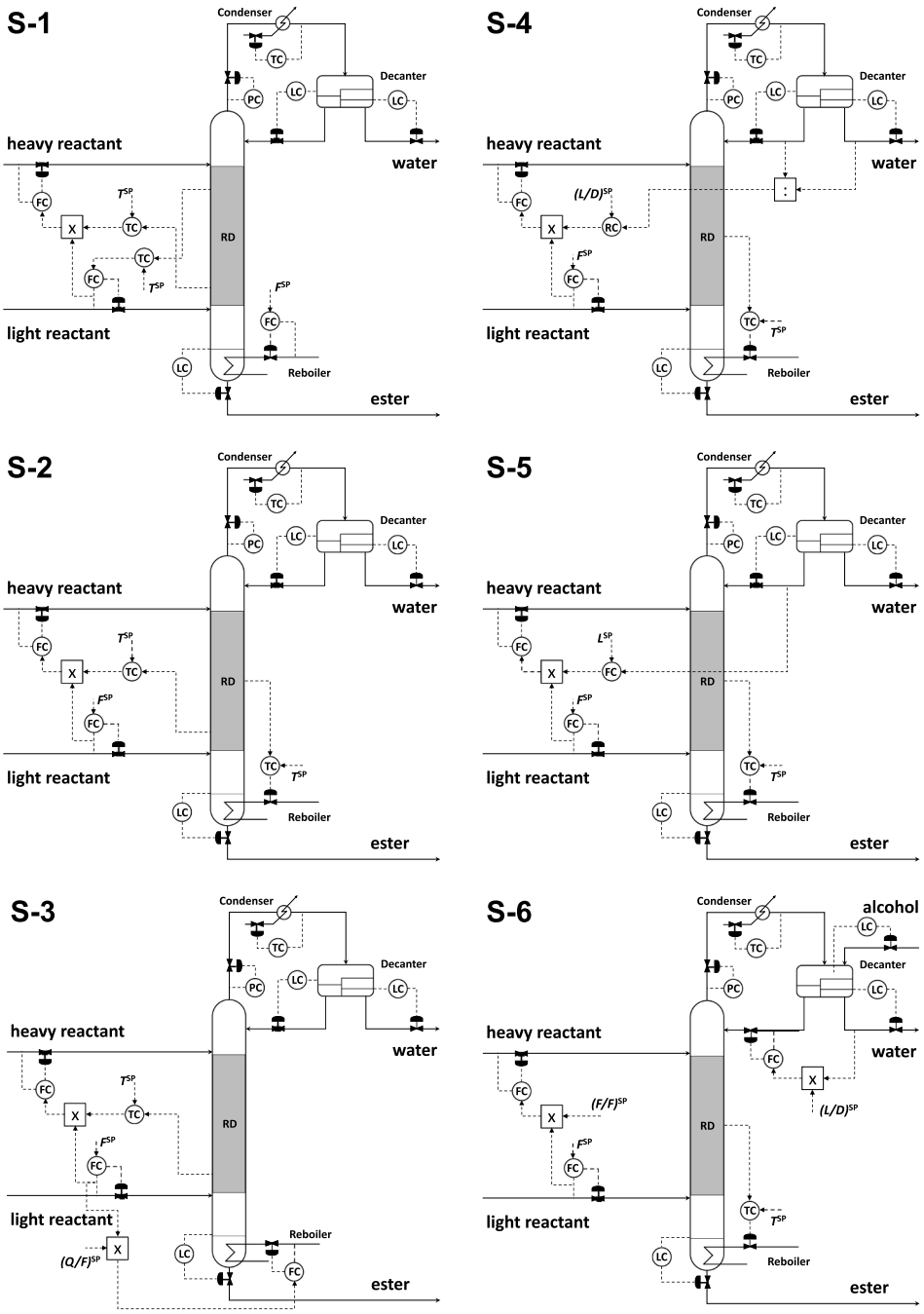

Fig. 1. Control of reactive distillation processes involving a heterogeneous azeotrope. Left – control structures presented in the literature. Right – new control structures proposed by this work.

rate) is set, and the level of the organic phase is controlled by the alcohol.

The idea of fixing the reflux rate and using the level in the reflux drum as indication of the inventory of one of the reactants was also applied by Al-Arfaj and Luyben [30] to ethylene glycol reactive distillation column, a process which involves two reactants (water and ethylene oxide), but only one product (ethylene glycol). The authors point out that this structure should be generally applicable to other similar systems. Our paper proves that it can be extended to heterogeneous reactive distillation.

Regarding control structures S-4, S-5 and S-6 we note that other combinations are possible, for example using the heavy reactant to set the production rate and ensuring the feed of the reactants in the stoichiometric ratio by using the flow rate of the light reactant to control either the reflux rate or reflux ratio. The applicability of the idea is not restricted to the arrangements shown in Fig. 1 (right column), as it will be shown in the case studies.

3. Methodology and approach

The performance of the new control structures is evaluated and compared to the literature ones by means of several case study. Aspen Plus and Aspen Plus Dynamics are used as efficient computer-aided process engineering tools for rigorous simulations. The next section presents the process design, including the mass balance and the main sizing elements. In all cases, the columns where sized using the "internals" facility offered by Aspen Plus. The vessels are designed to ensure 10 min residence time.

PI control is used in all cases. For the temperature control loops, a measurement deadtime of 1 min is considered. The temperature controllers are tuned by finding the ultimate gain and the period of oscillations at stability limit by the ATV technique and using the Tyreus-Luyben settings. In only a few cases, the Ziegler-Nichols settings are applied to have a more aggressive controller. For S-1 and S-2, in which two temperature controllers are involved, each temperature loop is tuned one at a time, and the procedure is repeated until no difference in the controller parameters is obtained. For the level and the other temperature controllers (i.e., condenser and evaporator) the gain is set to 1%/%, while the integral time is set to 60 min. and 12 min., respectively. For the pressure controllers, the gain is set to 2%/% and the integral time to 12 min. Note that the flow-driven dynamic simulation employed here assumes that well-designed pumps, control valves and flow controllers allow setting mass flow rates to desired values, without explicitly including these items in the simulation model. Detailed process control schemes and tuning of the most important controllers are given in the *Supplementary Material*.

The performance of the six control structures presented in Fig. 1 is evaluated by means of dynamic simulation performed in Aspen Plus Dynamics. Four different disturbances are considered, namely increase or decrease of the production rate by 25%, and contamination of the reactants (one at a time) by 5% mass water. The results of the dynamic simulations are shown in similar plots, which facilitates comparison of the results.

- **Case study 1**, 2-ethylhexyl acrylate process: amongst the reactants, acrylic acid is the light component (n.b.p. 141 °C), while 2-ethylhexanol is the heavy component (n.b.p. 184 °C) forming a low-boiling heterogeneous azeotrope with water. There is a large gap between the n.b.p. of the heavy reactant and that of the product (ester, n.b.p. 214 °C)
- **Case study 2**, n-butyl acrylate process, involves reactants with different ordering of the boiling point, namely the alcohol (n-butanol) is the light component (n.b.p. 118 °C), while the acid is the heavy component (n.b.p. 141 °C). The ester (n.b.p. 145 °C) is close to the heavy reactant. A particular feature is the rather high solubility of the alcohol in water. Thus, the aqueous phase resulting from the decanter contains important amounts of n-butanol. This is separated in a flash and recycled.
- **Case study 3**, n-butyl acetate process, involves reactants with very close boiling points (acetic acid, 117.9 °C, butanol 117.7 °C). Moreover, the reactants form a high-boiling homogeneous azeotrope (n.b.p. 122.5 °). Thus, the reactants are fed close to the top of the reactive section.
- **Case study 4**, amyl acetate process, is similar to case study 1 (2-ethylhexyl acrylate): amongst the reactants, acid is the light component (n.b.p. 118 °C), the alcohol is the heavy component (n.b.p. 138 °C). However, both reactants are fed as liquid close to the top of the reactive section. The column lacks a rectifying section.
- **Case study 5**, simultaneous n-butyl acetate and amyl acetate process is a two-column design, reactive distillation followed by separation of the esters in a conventional distillation column. The reactants are fed close to the top of the RD column, the column lacks a rectifying section, and the organic phase resulting from the decanter is refluxed.

4. Results and discussions

In this section, the performance of the new control structures is evaluated and compared to the literature ones by means of case studies. For each example, we provide the basic information regarding chemistry, thermodynamics and kinetics. The process layout is also shown such that the readers can easily find the basic data in case they want to reproduce the results.

4.1. Case study 1: 2-ethylhexyl acrylate

2-Ethylhexyl acrylate (*2*-EHA) is an important bulk chemical used as precursor in the production of acrylic polymers. Industrially, *2*-EHA is produced from acrylic acid (AA) and *2*-ethylhexanol (*2*-EH), catalysed by strong acidic catalysts. In this esterification reaction, water is formed as by-product.

In a previous paper [7], we described in detail the design of a reactive-distillation process for *2*-EHA production (20 kt/yr, 99.5% mass purity), employing Amberlyst 70 as solid catalyst. Here, we present only a short summary of the kinetics, thermodynamics and the main process design elements. The reaction rate (r, kmol/(kg_{cat}·s)) of *2*-EHA production is described by a pseudo-homogeneous kinetic model, Eqs. (1) and (2), using component activities. The pre-exponential factor k_0 is 722.7 kmol/(kg_{cat}·s), the activation energy E_A is 51.77 kJ/mol, while the two constants in the equilibrium constant equation (K_{eq}, activity-based) are $A = -8.5845$ and $B = 2438.5$ K.

$$r = k_0 \exp(-E_A/(RT))\left(a_{acid}a_{alcohol} - \left(1/K_{eq}\right)a_{ester}a_{water}\right) \quad (1)$$

$$\ln\left(1/K_{eq}\right) = A + B/T \quad (2)$$

All physical properties required in the process calculations are rigorously modelled using the UNIQ-HOC thermodynamic method in Aspen Plus and its default models. This method uses the UNIQUAC activity coefficient model to describe the behaviour of the liquid phase, while the vapour phase is described using the Hayden-O'Connell (HOC) equation of state, including the chemical theory of dimerization to account for the dimerization of acrylic acid. The model parameters for calculating the pure component properties are all available in the Aspen databanks. Three sets (water/AA, water/*2*-EH, and AA/*2*-EH) of the binary interaction parameters for the UNIQUAC model are present in the Aspen databanks. The other three sets (water/*2*-EHA, AA/*2*-EHA, and *2*-EHA/*2*-EH) are estimated using the UNIFAC predictive model. The association parameters for the binary AA/water used by the HOC model are also available. Details on the thermodynamics of this system are presented in the previous paper [7] and the references therein.

The process flow diagram, mass balance (stream composition as mole fractions) and main operating parameters, together with the main equipment dimensions used for holdup calculations, are presented in Fig. 2. Fresh *2*-EH liquid is fed at the top of the catalytic bed (stage 3). Fresh AA is vaporized and fed below the catalytic bed (stage 17). The top vapours are condensed, and then phase separated in the decanter. The organic phase of the decanter is returned as reflux to the column (stage 1), while the aqueous phase (99.9% mass water) is removed from the process.

The six control structures described in detail in Section 2 are tested on this process. The *Supplementary Material* presents a detailed implementation of each control structure. For easy identification, the numbering is the same as previously presented. Using the temperature profile along the column, the slope criteria (i.e., $\Delta T = T_{n+1}$-T_n, where T is the temperature and n is the stage number) indicates stages 4, 17 or 21 as suitable for temperature control. For control structures S-1 and S-2, which require two temperature measurements, various combinations were tested. Namely, for S-1, temperature on stage 4 is controlled by manipulating the flow rate of fresh acid, while temperature on stage 21 is controlled by the ratio between the two fresh feed flows. For S-2, the temperature on stage 4 is controlled by manipulating the reboiler duty, while the other temperature control loop is the same as in S-1. For the remaining control structures, one temperature in the stripping section (stage 21) is selected, as it provides the tightest control of the bottom purity.

Fig. 3 presents dynamic simulation results, comparing the performance of the literature and new control structures for several process changes. All these results represent the product purity (% mass of acrylate in the bottom product stream). Note that the purity of the

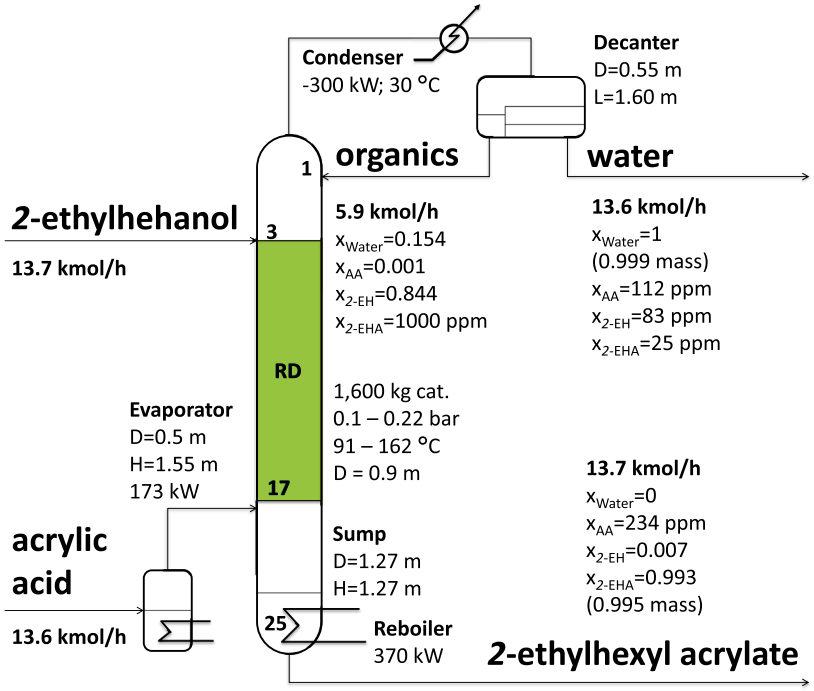

Fig. 2. Process design results for 2-ethylhexyl acrylate production. When CS-6 is applied, 12.4 kmol/h of 2-ethylhexanol are fed in the column, and 1.3 kmol/h in the decanter.

aqueous stream hardly notes any changes, the water practically remaining at the steady-state value of 99.9% mass (results not included). The results of the ester purity are arranged as follows:

- The graphs on the left column capture the process behaviour using the literature control structures, while the graphs on the right column capture the behaviour using the proposed control structures.
- The graphs on each row capture the process behaviour subjected to a different process change; or differently said, one row per one process change.

There are four process changes testing the control structures, each process change being introduced one at a time. At the start of the simulation the process is in steady state, and the steady state is maintained for 2 h. Then, the process change is introduced as a ramp-change for 1 hour time interval. The first process change is the increase in the production rate with 25%. As previously described, except for S-1, this is achieved by increasing the flow rate of fresh acid by 25%. S-1 achieves this by increasing the reboiler duty by roughly 20%. The results are captured by the top graphs. A new stationary regime is reached in about five hours. Among the literature control structures, S-1 is the best performing, closely followed by S-2 and S-3. Among the new control structures, S-5 shows the best results, practically having the same performance as S-1 in terms of speed of disturbance rejection and offset in product purity. S-6 follows closely and is comparable in performance with S-2 and S-3, while S-4 shows the highest offset. Note that S-4 and S-5 show a large offset of the purity during the transition period, from one steady state to the other. Nevertheless, none of the control structures is able to keep the product purity at the value of 99.5% mass, despite the fact that the set-points of the temperature controls are maintained.

The second process change is the decrease in the production rate with 25%. This is achieved in a similar way as in the previous process change. Except for S-1, the production is decreased by decreasing the flow rate of fresh acid by 25%. S-1 achieves the decrease in production by decreasing the reboiler duty by 20%. The results are captured by the middle-top graphs. The new stationary regime is reached very soon after the change is implemented. Practically, all control structures have the same performance. The product has a slight increase in purity.

The third process change is the contamination of fresh acid with water, from 0 to 5% mass. The results are captured by the middle-bottom graphs. The response is practically the same. All structures show only a slight decrease in product purity; S-6 presents the largest offset, but close to that showed by the other control structures.

The last process change is the contamination of fresh alcohol with water, from 0 to 5% mass. The results are captured by the bottom graphs. The best performing control structures are S-1, S-2 and S-3; practically, all have the same response and are able to maintain the product purity close to the required value of 99.5% mass. The closest performance is that of S-5, achieving a product purity of 99% mass. S-6 achieves a product purity of 98.8% mass; however, during the transition period from one steady state to the other, the purity decreases for some period of time down to 94% mass. S-4 has the largest offset in product purity and a large decrease in purity during the transition period.

For all control structures, the production rate increase is the most difficult process change to cope with. The vapour-liquid traffic in the column increases when more reactants are fed to the process. This results in a higher pressure at the bottom of the column, and even if the temperature is maintained at its set-point, the product purity is no longer ensured. For this reason, the set-point of the temperature controller can be compensated according to a linear pressure-temperature relationship. The performance of this extended control structure is shown for S-5 (i.e., S-5*). The results are excellent, all disturbances being rejected with small overshoots, low settling time and almost no composition offset. This extension is applicable to all control structures.

4.2. *Case study 2: n-butyl acrylate*

n-Butyl acrylate (*n*-BA) is an important bulk chemical used as precursor in the production of acrylic polymers. Industrially, *n*-BA is produced from acrylic acid (AA) and *n*-butyl alcohol (BuOH), catalysed by strong acidic catalysts; in this reaction, water is formed as by-product.

In a previous paper [6], we described in detail the design of a reactive-distillation process for *n*-BA production (20.6 kt/yr, 99.5%

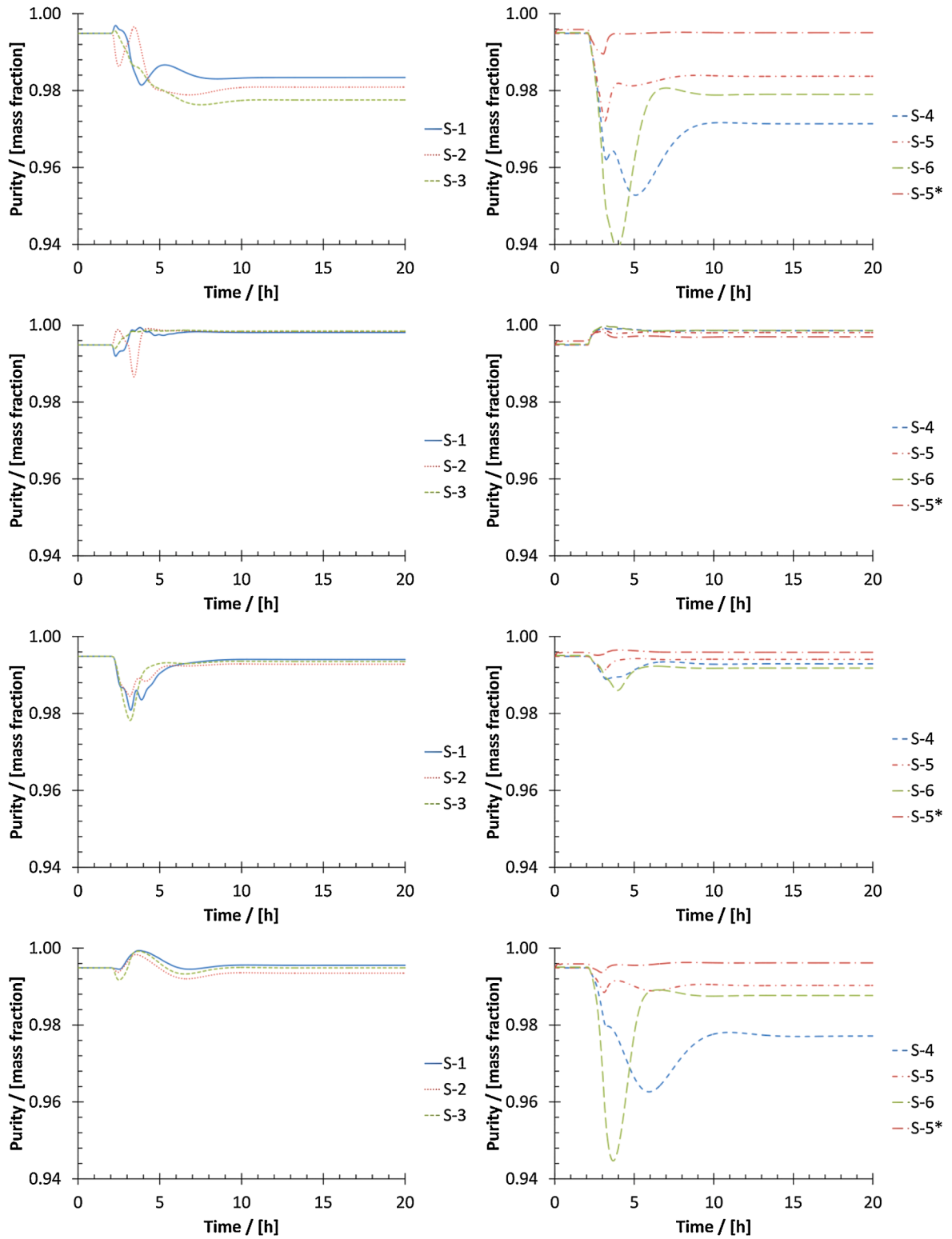

Fig. 3. *2*-Ethylhexyl acrylate process dynamics associated with each control structure (left column: literature structures S-1, S-2, S-3; right column: novel structures S-4, S-5, S-6) at various process changes: top diagrams: +25% production; middle-top diagrams: −25% production; middle-bottom diagrams: 5% mass water in fresh acid; bottom diagrams: 5% mass water in fresh alcohol.

mass purity), employing Amberlyst 131 as solid catalyst. Here, we present only a short summary of the kinetics, thermodynamics and the main process design elements detailed in the aforementioned paper. The reaction rate (r, kmol/s) of *n*-BA production is described by the Langmuir-Hinshelwood-Hougen-Watson kinetic model proposed by Sert et al. (2013). The model described by Eq. (3)-(6) uses component activities. The rate constant of the forward reaction (k_f, kmol/kg_{cat}·s) is described by the Arrhenius Eq. (4): the pre-exponential factor k_0 is 227, 522 kmol/(kg_{cat}·s) and the activation energy E_A is 57.4 kJ/mol. The two constants in the equilibrium constant equatiosn (K_{eq}, activity-based) are $A = -1.799$ and $B = 2134$ K. The parameters C_i and D_i of the adsorption constant equation, K_i (i = acid, alcohol, ester and water), are given in

Table 1
Parameters of the adsorption constant for each component (Eq. (6)).

Component		Water	BuOH	AA	*n*-BA
Parameter	C	−2.0325	−4.4473	−6.4719	−4.4937
	D / [K]	1340.6	1498.1	2235.8	1107.0

Table 1. m_{cat} (kg_{cat}) is the mass of catalyst.

$$r = \frac{m_{cat} k_f K_{acid} K_{alcohol} \left(a_{acid} a_{alcohol} - \left(1/K_{eq}\right) a_{ester} a_{water}\right)}{\left(1 + K_{acid} a_{acid} + K_{alcohol} a_{alcohol} + K_{ester} a_{ester} + K_{water} a_{water}\right)^2} \quad (3)$$

$$k_f = k_0 \exp\left(-\frac{E_A}{RT}\right) \quad (4)$$

$$K_{eq} = \exp(A + B/T) \quad (5)$$

$$\ln(K_i) = C_i + D_i/T \quad (6)$$

Two thermodynamic methods, UNIQ-HOC and UNIQ-2 (default naming in Aspen Plus) with their constituting property models, are used to calculate the phase equilibria and all the other physical properties required in simulating the process. While UNIQ-HOC is used by most of the simulation blocks, UNIQ-2 is set-up to appropriately describe the liquid-liquid equilibria in the decanter. Therefore, while both methods use the same activity coefficient model (i.e., UNIQUAC), some of the binary interaction parameters sets are different. All the interaction parameters are those used by Niesbach et al. [31]; note that all parameters are available in the Aspen Plus database, except for those of water/*n*-BA and AA/*n*-BA pairs.

The process flow diagram, mass balance and main operating parameters, together with the main equipment dimensions used for holdup calculations, are presented in Fig. 4. Fresh AA liquid is fed at the top of the catalytic bed (stage 5). Fresh BuOH is vaporized and fed below the catalytic bed (stage 25). The top vapours are condensed, and then phase separated in the decanter. The organic phase of the decanter, containing important amounts of alcohol, ester and water, is returned as reflux to the column (stage 1), while the aqueous phase is sent to a flasher for alcohol recovery. This is possible due to the minimum boiling azeotrope of water/alcohol; namely, by vaporizing the azeotrope and recycling it to the column (stage 7).

The six control structures (see the *Supplementary Material* for details) are tested also on this process. For easy identification, the numbering is the same as previously presented. The slope criteria indicates stages 1, 7 or 26 as suitable for temperature control; since on stages 1 and 7 the recycle and, respectively, the reflux streams are added, these stages are not considered for temperature control; instead, stages 2 and 8 are selected since the difference in temperature is relatively large. For S-1, temperature on stage 26 is controlled by manipulating the flow rate of fresh acid, while temperature on stage 2 is controlled by the ratio between the two fresh feed flows. For S-2, the temperature on stage 26 is controlled by manipulating the reboiler duty, while the temperature on stage 8 is controlled in the same way as in S-1; poorer performances are obtained when using stage 2 for temperature control. For the remaining control structures, one temperature in the stripping section (stage 26) is selected, providing the tightest control of the bottom purity. For all control structures, flash temperature, pressure and liquid level are controlled by duty, vapour and liquid flow rates, respectively.

Fig. 5 presents dynamic simulation results, comparing the performance of the literature and new control structures for several process changes. These results represent the purity of both outlet product streams of the process (ester and water). The results are arranged as follows:

- The graphs on the left column capture the process behaviour using the literature control structures, while the graphs on the right column capture the behaviour using the proposed control structures.
- The graphs on each row capture the process behaviour subjected to a different process change; or differently said, one row per one process change.
- Each two-graphs collection (note: there are 8 two-graphs collections in total) shows the % mass of ester in the bottom stream of the column (i.e., the *ester* graph) and the % mass of water in the liquid stream of the flasher (i.e., the *water* graph).

There are four process changes testing the control structures: increase in production capacity by 25% (top graphs), decrease in capacity by 25% (middle-top graphs), contamination of fresh acid with water,

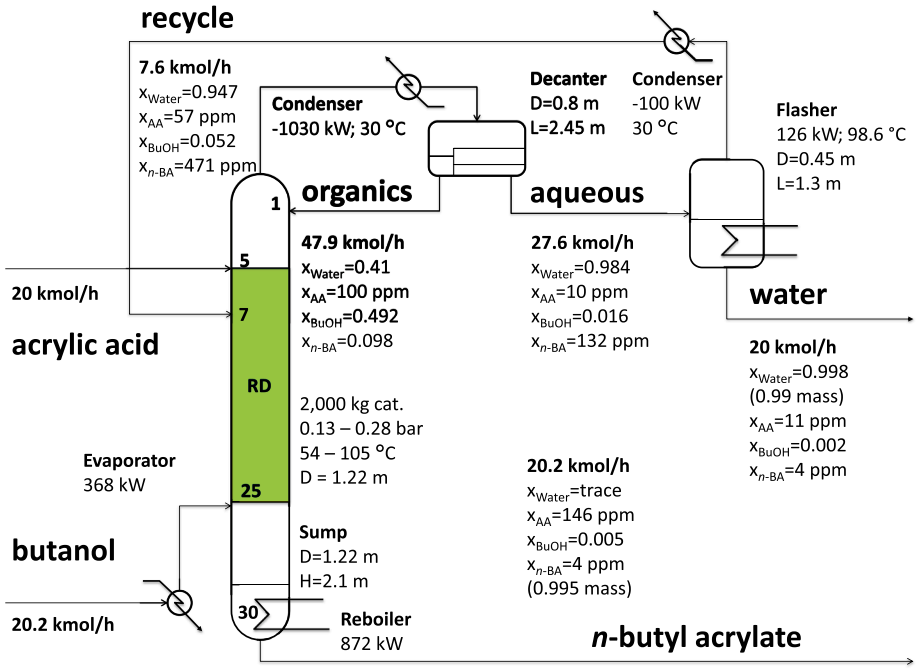

Fig. 4. Process design results for *n*-butyl acrylate production. When CS-6 is applied, 13.4 kmol/h of n-butanol are fed in the column, and 6.6 kmol/h in the decanter.

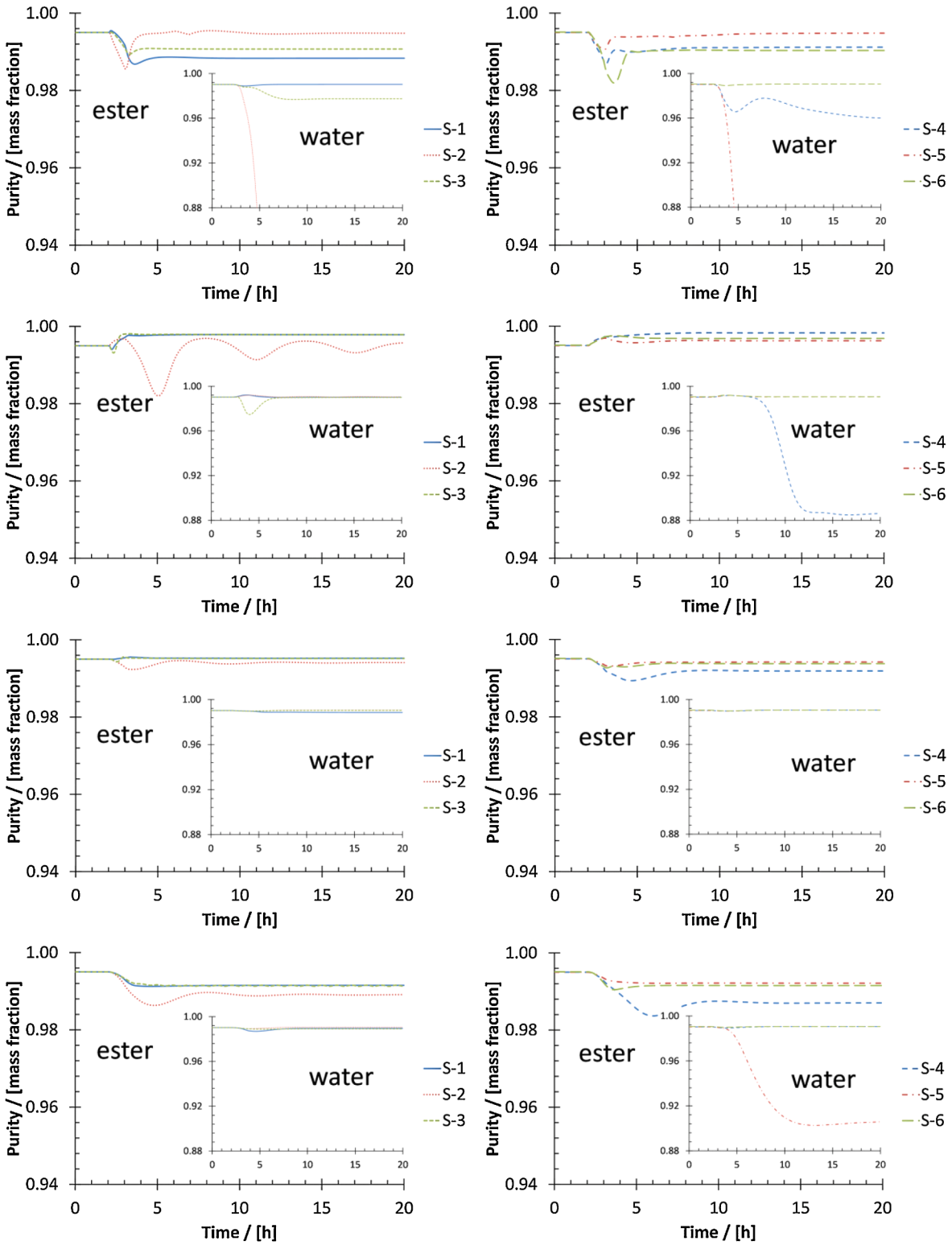

Fig. 5. *n*-Butyl acrylate process dynamics showing the purity of the ester (larger graphs) and water (smaller graphs) product streams associated with each control structure (left column: literature structures S-1, S-2, S-3; right column: novel structures S-4, S-5, S-6) at various process changes: top diagrams: +25% production; middle-top diagrams: −25% production; middle-bottom diagrams: 5% mass water in fresh acid; bottom diagrams: 5% mass water in fresh alcohol.

from 0 to 5%mass (middle-bottom graphs) and contamination of fresh alcohol with water, from 0 to 5% mass (bottom graphs). As in the previous case study, each process change is being introduced one at a time, following the same procedure (i.e., at the start of the simulation the process is in steady state, and the steady state is maintained for 2 h; then, the process change is introduced as a ramp-change for 1 hour time interval).

Remarkable, for all process changes, all control structures keep the ester product stream at high purity, and only small differences between their results are observed (i.e., some purity off-sets and some struggle to transition to a new operating point with somewhat larger settling time). However, when looking at the purity of the water product stream, some

of the structures fail in maintaining the high purity. For 25% increase in capacity, the control structures S-2 and S-5 fail, the purity falling to roughly 43% mass (not captured by the graphs), while S-3 and S-4 are levelling-off around a purity of 98 and 96% mass, respectively. S-4 also fails to keep a high purity when decreasing the capacity by 25%, while S-5 also fails when the fresh alcohol is contaminated by 5% mass water; in both situations, the water purity drops down to around 90% mass.

In all situations, the drop in water purity is due to the acid escaping in the top of the column. After condensation of vapours, the acid is distributed in both organic and aqueous phases of the decanter (note that the acid is completely miscible with both alcohol and water). Thus, the aqueous stream feeding the flasher contains significant amounts of acid. Since the acid is the component with the highest boiling point, the boiling point of the mixture is increased making unfeasible the recovery of water at high purity. Hence, preventing the acid to escape in the overhead of the column is a key element in achieving high-purity water.

Control structures S-1, S-3 and S-6 can keep high purity set-points of both the ester and water product streams for all the process changes tested in this study.

4.3. Case study 3: n-butyl acetate

n-Butyl acetate is an essential solvent for chemical industry, largely used for plastics, liquors, resins, gums, and coatings. Due to its low toxicity, which makes it an environmentally friendly compound, it can replace a toxic solvent (e.g., ethoxy ethyl acetate). *n*-Butyl acetate can be synthesized through esterification of acetic acid with butanol in the presence of ion-exchange resin catalysts (Amberlyst 15). [32] presents vapour – liquid – equilibria data compiled from various sources. These data, together with data retrieved from the NIST database are regressed to find the binary interaction parameters of the NRTL-HOC thermodynamic model. The experimental data provided by Gangadwala et al. [33] are used to regress the parameters of a power-law kinetic model:

$$r = m_{cat}(k_1 a_{acid} a_{alcohol} - k_2 a_{ester} a_{water}) \quad (7)$$

The values of the regressed pre-exponential factors and activation energies used in our work are $k_{1,0}$ = 749,979 kmol/(kg_{cat}·s), $E_{A,1}$ = 63,961 kJ/kmol (forward reaction) and $k_{2,0} = 3.587 \cdot 10^8$ kmol/(kg_{cat}·s), E_A = 90,979 kJ/kmol (reverse reaction). Fig. 6 shows the process flow diagram and the key design parameters for butyl acetate production. The reactive distillation column contains 34 stages (where reactive section is from stage 5 to stage 24). The fresh acetic acid is fed in the top of the reactive section (stage 5). The butanol enters the column in the middle of the reactive section (stage 9). The vapours from the top of the column are condensed at 40 °C and the heterogeneous azeotropic mixture is separated in the decanter. The organic phase returns as reflux in the column, and the aqueous phase which contains mainly water is withdrawn with 93.3% mass purity. The butyl acetate is obtained as bottom product of reactive distillation column, with 99.5% mass purity.

The dynamics of this process was studied by Luyben and Yu [13], which compared the performance of structures S-1 (F-FR) and S-2 (Q-FR). For an increase of production of 20%, S-2 outperformed S-1, showing a lower settling time, although both structures would achieve the same steady-state results.

As in the previous case studies, all six control structures are used to control the process and tested for all four process changes. In the control structures S-1 and S-2, the ratio between the reactants is used to control the temperature on stage 1 and 6, respectively. In the other control structures, the temperature on stage 29 is controlled by means of reactants ratio (S-3) or reboiler duty (S-4, S-5, S-6, S-7). The results are presented in Fig. 7 and are arranged in the same way as for the case study presented earlier (i.e., +25% production rate in the top graphs, −25% production rate in the middle-top graph, 5% mass water in acid fresh feed in the middle-bottom graph, and 5% mass water in butanol fresh feed in the bottom graph).

In this case study, a new control structure, namely S-7 (which is an improvement of S-5), is briefly analysed; ignore for now the results of S-7 in Fig. 7.

For +25% capacity all structures, except for S-5, give comparable overall results:

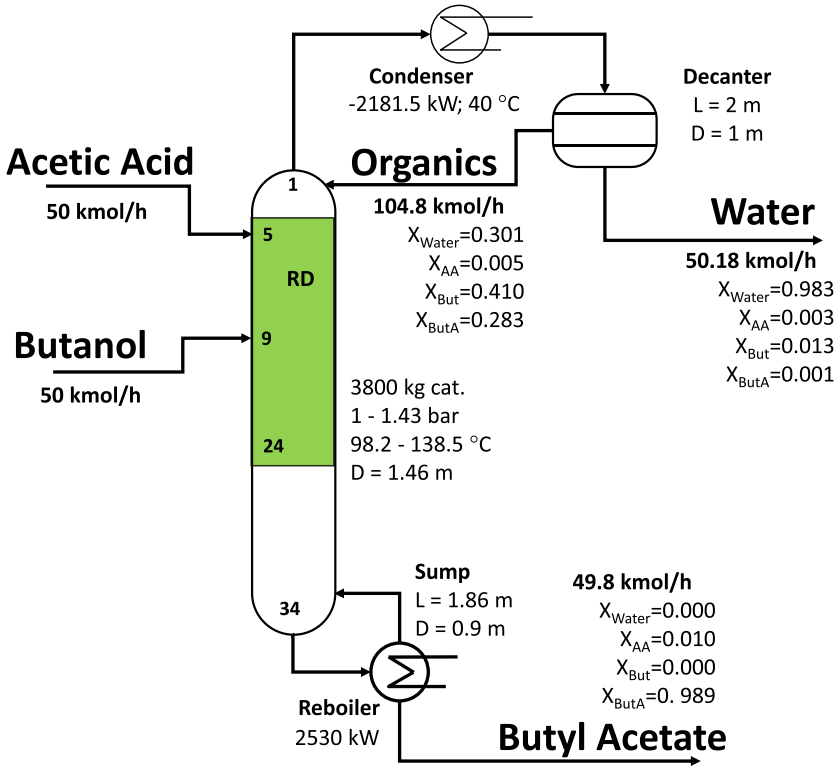

Fig. 6. Process design results for n-butyl acetate production. When CS-6 is applied, 36.5 kmol/h of butanol are fed in the column, and 14.6 kmol/h in the decanter.

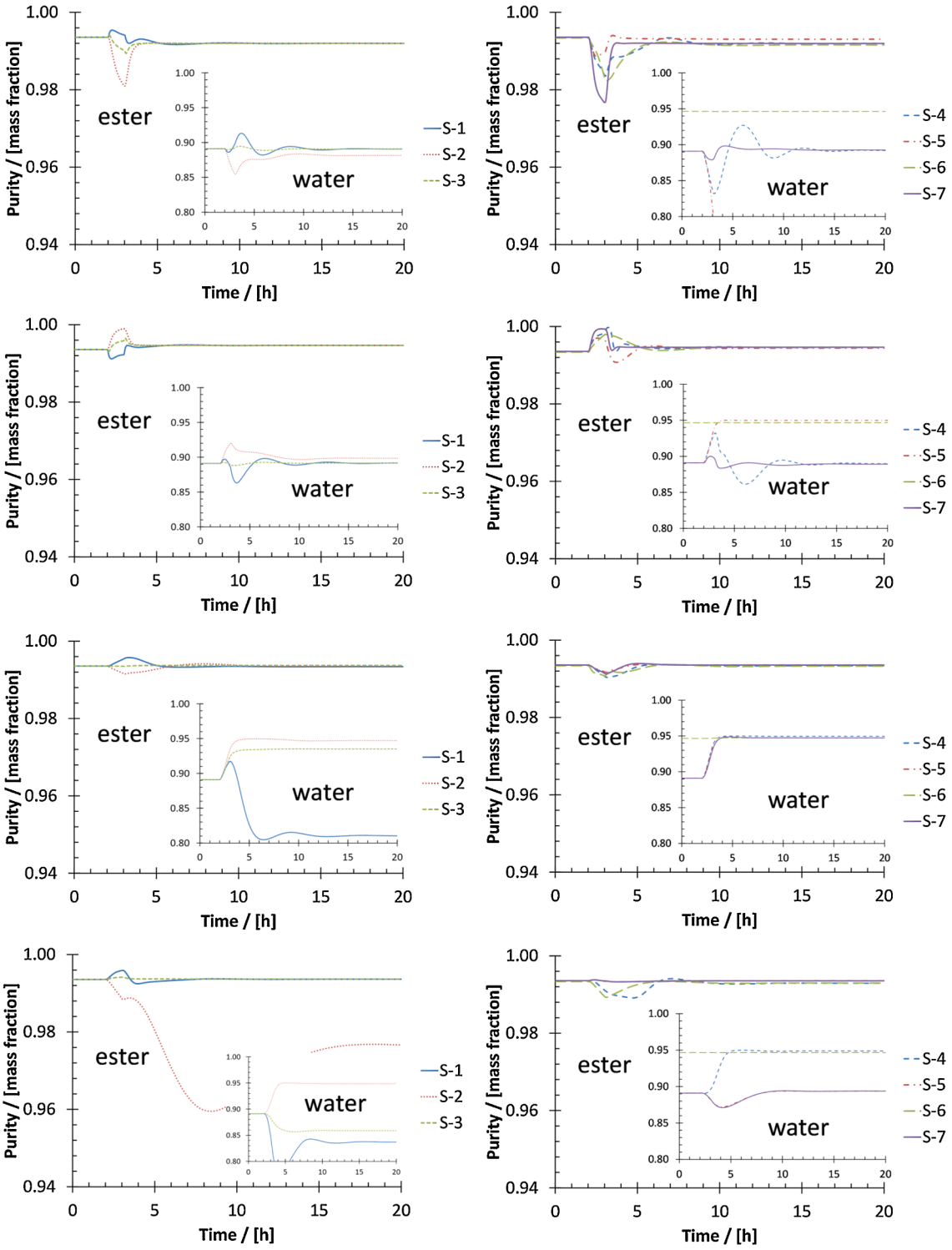

Fig. 7. Butyl acetate process dynamics associated with each control structure (left column: literature structures S-1, S-2, S-3; right column: novel structures S-4, S-5, S-6 at various process changes: top diagrams: +25% production; middle-top diagrams: −25% production; middle-bottom diagrams: 5% mass water in fresh acid; bottom diagrams: 5% mass water in fresh alcohol.

- The same ester purity is achieved by all structures, with some peak error during ramping-up the capacity; S-4 and S-6 show a slightly longer settling time.
- S-1, S-3 and S-4 achieve the same water purity; S-2 shows only a slight off-set; S-4 shows both, larger peak error and settling time. Since the process controlled by S-6 contains a second fresh alcohol stream fed in the decanter, the starting water purity is higher, and S-6 maintains the same purity during the transition period.
- Although S-5 maintains the ester purity at the high values, if fails to control the water purity (dropping to 65% mass), the stream becoming contaminated mainly with acid and some acetate. This failure is attributed to the organic reflux – fresh feeds ratio control

loop, since is cannot detect the acid exiting the process with the water stream.

In contrast to the results obtained by Luyben and Yu [13], the results we obtain show that S-1 outperformed S-2. One explanation might be the addition of fresh reactants: In the design of Luyben and Yu [13], the alcohol is fed on a stage above the addition of the acid, while in our study is the other way around. Nevertheless, the differences are practically small.

At −25% capacity, about the same results are obtained as for increase in production. The exception is the results of S-5, which is able as well to maintain at high purity both the ester and water products.

When the fresh acid feed is contaminated with 5% mass water, all structures have the same results regarding the ester purity. The purity of water shows an increase (and about the same) for all structures, excepting S-1. For this structure, the water purity drops down from 89 to roughly 81% mass. When the fresh alcohol is contaminated with 5% mass water all structures, excepting S-2, are able to maintain the high ester purity and show very small peak errors and small settling times. The results of S-2 show large purity off-set, peak error and setting time.

Regarding the water product, the results vary widely:

- In the case of S-1 and S-3, the water purity drops down from 89 to roughly 84–86% mass, respectively. S-1 shows a relatively large peak error and settling time.
- For S-2 and S-4, the water purity shows an increase close to 95% mass.
- For S-5, the water purity remains the same, with a small peak error; for S-6, the purity starts from a higher value (due to the second fresh alcohol feed) and remains at the same value throughout the process change.

The additional control structure S-7 controls the reflux / feed (L/F) ratio manipulating the ratio of the fresh reactants, as opposed to S-5 in which the reflux (L) alone is controlled. S-7 has the advantage of directly taking into account the increase / decrease in capacity by measuring the throughput manipulator (i.e., the fresh acid feed). Note that if the feed flow rate does not change, then S-7 achieves the same results as S-5. Overall, for this specific case study and process changes tested, S-7 outperforms all the other control structures, showing relatively small peak errors and settling times.

4.4. Case study 4: amyl acetate

Amyl acetate is considered an important solvent, extractant, or polishing agent with wide application in different industries such as food, cosmetics, chemical and pharmaceutical. It can be synthesized from acetic acid and amyl alcohol via an esterification reversible reaction in the presence of a solid acidic catalyst (Amberlyst 15). The reaction rate given in Eq. (8) is described by [32] as a quasi-homogenous model, expressed by concentrations. The pre-exponential factor of the forward reaction k_1 is 31.1667 kmol/kg$_{cat}$·s with an activation energy E_A of 51, 740 kJ/kmol. The reverse reaction has a pre-exponential factor k_2 of 2.2533 kmol/kg$_{cat}$·s, with an activation energy E_A of 45,280 kJ/kmol.

$$r = m_{cat}(k_1 C_{acid} C_{alcohol} - k_2 C_{ester} C_{water}) \quad (8)$$

The NRTL-HOC thermodynamic method in Aspen Plus is set-up for calculating the physical properties necessary in process simulations. The binary interaction parameters of the NRTL activity model are regressed form experimental data retrieved from the NIST database (via the NIST-TDE in Aspen).

Fig. 8 shows the process flow diagram and the key design parameters for the amyl acetate production. The reactive section contains 20 stages, from stage 1 to stage 20. The amyl alcohol is fed on stage 1 and the acetic acid is fed on stage 5, both in liquid phase. The amyl acetate is obtained as bottom product (stage 30) with 99.9% mass purity. The water is

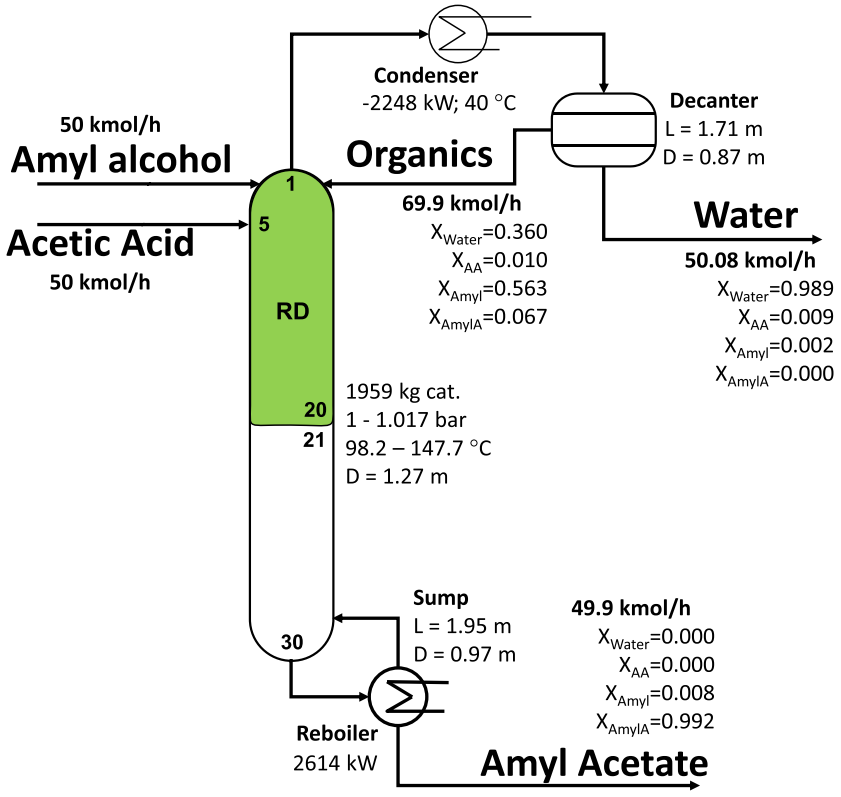

Fig. 8. Process design results for Amyl Acetate production. When CS-6 is applied, 38.6 kmol/h of amyl alcohol are fed in the column, and 11.4 kmol/h in the decanter.

obtained from the decanter with a purity of 98.1% mass. The organic phase is returned in reactive section of the column, on stage 1. Although our design is somewhat different, one can consult the designs of Luyben and Yu [13] and [32] for details regarding the RD applied to the amyl acetate process.

The most temperature sensitive are stages 2 and 22, which are used by all control structures. The performance of each control structure is shown in Fig. 9, arranged in the same way as in the previous case studies. Since the water purity practically does not change, for any of the control structures and process changes, these results are not presented. Regarding the purity of the ester product, all the control structures have good results, and only minor differences can be seen in their

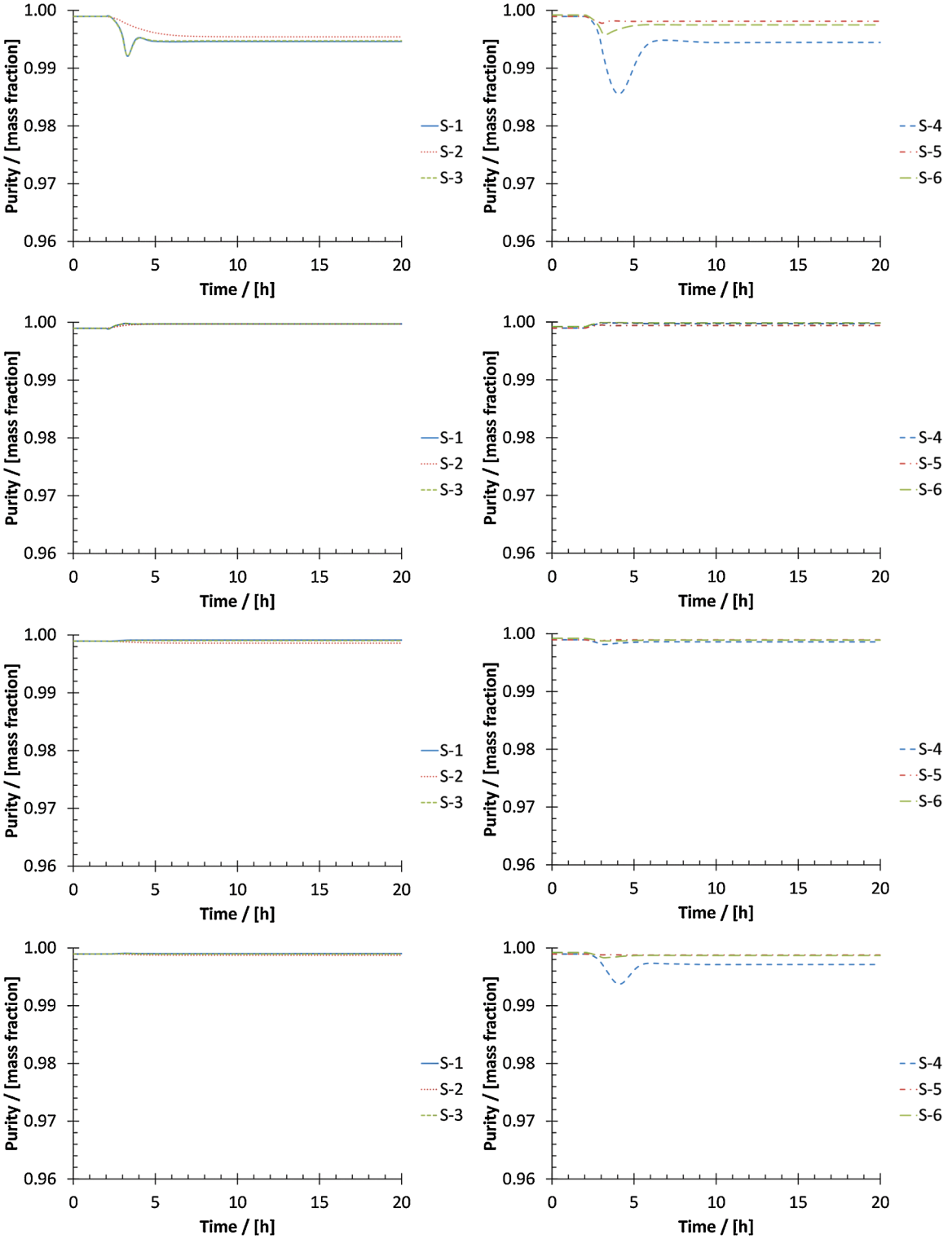

Fig. 9. Amyl acetate - process dynamics associated with each control structure (left column: literature structures S-1, S-2, S-3; right column: novel structures S-4, S-5, S-6) at various process changes: top diagrams: +25% production; middle-top diagrams: −25% production; middle-bottom diagrams: 5% mass water in fresh acid; bottom diagrams: 5% mass water in fresh alcohol.

performance.

The most difficult process change to cope with is the increase in capacity (+25%). The results for S-1, S-2, S-3 and S-4 are very similar, the purity of the ester product decreasing from 99.9 to 99.4–99.5% mass. The results show small peak errors and settling times, with the exception of S-4; for this structure, some larger peak error and settling time are observed. S-5 and S-6 are best performing, but not much better than the other ones.

There is practically no change in product purity for 25% decrease in production or when the fresh acid is contaminated with 5% mass water. When the fresh feed of alcohol is contaminated with 5% mass water, the purity of the amyl acetate product shows a decrease (from 99.9 to 99.7% mass) in the case of control structure S-4; a peak error is also observed.

4.5. Case study 5: mix of butyl acetate and amyl acetate

Amyl alcohol and butanol are considered wastes in the production of semiconductors and pharmaceutics products. Considering the value of the amyl acetate and butyl acetate for some industries (mentioned in previous sections), [32] developed two processes which use a reactive distillation column to produce two esters (amyl acetate and butyl acetate). One of the processes is used here, in our study. Note that the [32] process uses a rather large reactive distillation column (28 reactive stages, 88 stripping stages). Our design achieves the same production rate and purity with a much smaller stripping section column (23 stages). The reaction kinetics and thermodynamics data used are the same as mentioned in the butyl acetate and amyl acetate case studies inSection 4.3 and Section 4.4, respectively. More information about this process is given by [32].

The mass balance and the key design parameters are presented in Fig. 10. The mixture of alcohols is fed on stage 1, meanwhile the acetic acid is fed on stage 5. The mixture of butyl acetate and amyl acetate are obtained in the bottom of reactive distillation column (RD), then sent to a conventional distillation column (DC) for separation. The butyl acetate is obtained as distillate (98.9% mass), and the amyl acetate as bottom product (99.0% mass). In this process the organic phase is returned from decanter to the reactive column.

Hereafter, the control structures mentioned in Section 2 are applied (see the *Supplementary Material* for details). Following the same procedure as in previous cases, the temperature sensitive stages were found to be stage 3 and stage 29, which are used further for temperature control in the reactive distillation column. The control structure of conventional distillation column is kept the same for all cases: besides the usual pressure and level control, the temperature of stage 22 is controlled by manipulating the reflux rate, and the temperature of stage 26 is controlled by manipulating the reboiler duty.

The performance of all six control structures is shown in Fig. 11. This figure also includes the performance of S-7, but just ignore for the moment the results of this structure. The purity results recorded in the Fig. 11 concerns the mass fraction of amyl acetate and butyl acetate in the bottom product of reactive distillation column. The purity of the water product does not vary significantly (results not presented).

Independent of the process change, the purity of the acetates product stream barely changes from its initial steady state value in the case of control structures S-1, S-2 and S-3; thus, the results are exceptional, showing no peak errors or large settling times. For the other control structures, S-4, S-5 and S-6, the results are as follows:

- For production rate changed by ±25% (top graph, right), S-4 and S-6 show relatively low peak errors and settling time, but maintaining the desired product purity. S-5 fails to do that, the product stream becoming contaminated with acid; the purity drops towards 90% mass.
- For decrease in production by 25% (middle-top graph, left), S-4 shows a relatively high peak errors and struggles to reduce the purity off-set during operation; after 20 h of operation, the purity off-set still shows about 0.7% mass difference compared to the initial steady state. S-5 fails to keep the initial product purity, dropping from 99.5 to 94.9% mass, the product being contaminated with pentanol. S-6 has a large peak error during the ramp-down of the production and a few hours after, but the settling time is large and the purity slowly comes back closer to the initial product purity; after 20 h of operation, the purity difference is about 0.3%, but the process did not yet reach the new steady state.
- In the case of fresh acid contaminated with 5% mass water, S-4 and S-6 show relatively small peak errors, but the settling time is large; the

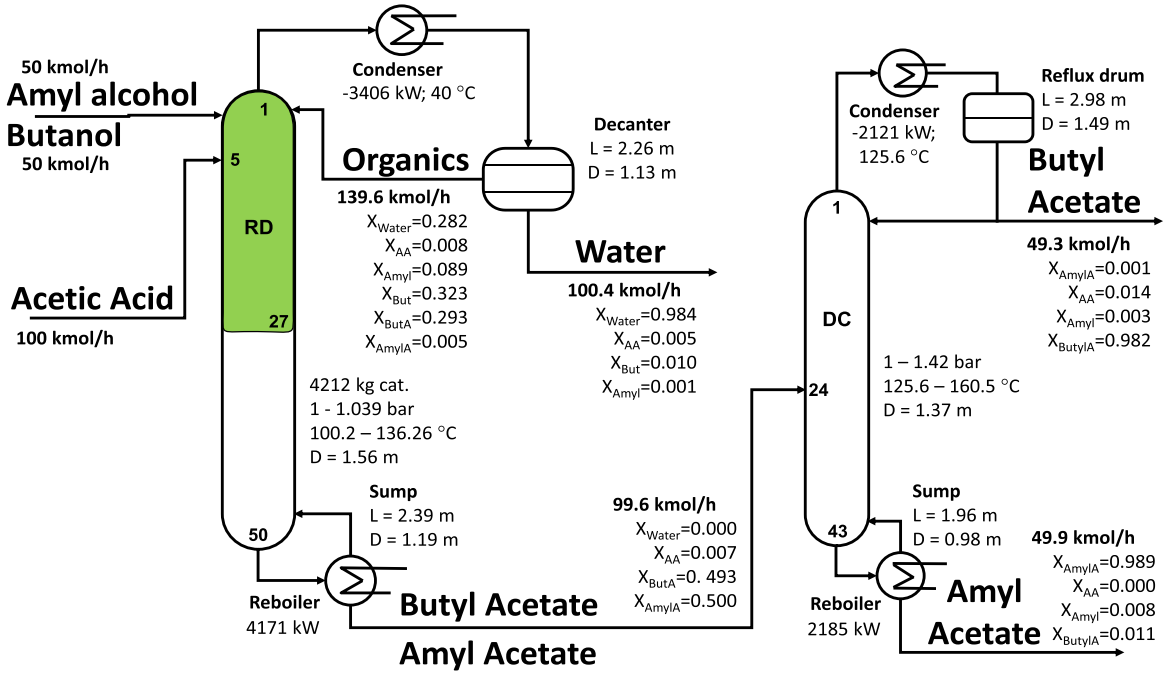

Fig. 10. Process design results for butyl acetate and amyl acetate production. When CS-6 is applied, 75 kmol/h of alcohols mixture (50/50%) fed in the column, and 25 kmol/h (50/50%) in the decanter.

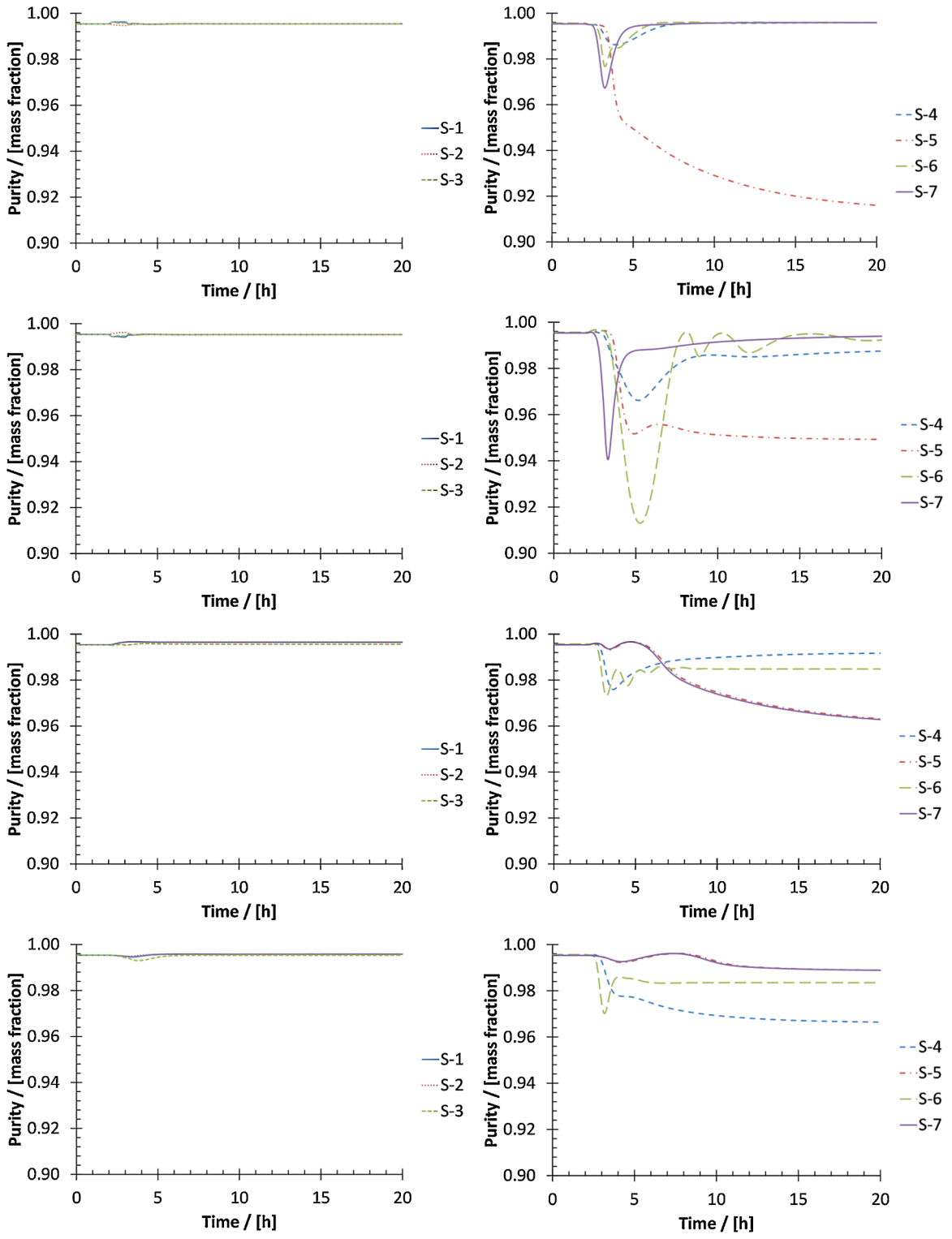

Fig. 11. Amyl acetate – butyl acetate mixture process dynamics associated with each control structure (left column: literature structures S-1, S-2, S-3; right column: novel structures S-4, S-5, S-6) at various process changes: top diagrams: +25% production; middle-top diagrams: −25% production; middle-bottom diagrams: 5% mass water in fresh acid; bottom diagrams: 5% mass water in fresh alcohol.

purity off-set is about 0.3% for S-4 and 1% for S-6. The results of S-5 show that the process did not reach a new steady state in 20 h of operation; a large product purity off-set (more than 4% mass) is observed after 20 h.

- When the fresh alcohol is contaminated with 5%mass water, the results of S-4 show a drop in product purity of 3% mass, failing to control the process. S-5 shows relatively small peak error, a large settling time, but a relatively low purity off-set of 0.6% mass. S-6 shows a relatively small peak error and settling time, but a purity off-set of 1.1% mass.

The performance of control structure S-7 is good for increase in capacity, showing relatively small peak error and settling time, and no off-set in product purity. However, for decrease in production capacity, the

results show a larger peak error, while the off-set of the product purity slowly decreases during 20 hour of operation due to the large settling time of the L/F ratio controller. As expected, for the process changes in which the water contaminates the fresh acid / alcohol stream, S-7 exhibits the same behaviour as S-5.

5. Conclusions

This paper proposes a novel class of control structures applicable to heterogeneous reactive distillation. The production capacity and purity of the bottom product are achieved in the same way as largely accepted in the literature. However, balancing the reaction stoichiometry and controlling the reactants inventory by measuring flow rates, such as the organic reflux rate, or the organic reflux / aqueous distillate ratio, is a key novelty of this study (in contrast to the literature control structures, which, invariably, use temperature measurements for this purpose). Thus, when the reactant involved in the heterogeneous azeotrope is not fed in the correct amount, it will either accumulate in the system (case in which the reflux increases) or get depleted (reflux decreases). The basic concept can be implemented in various ways as clearly demonstrated by the case studies presented. These case studies covered five esterification systems of industrial importance and a wide range of operating conditions.

The performance of the new control structures is compared with that of the literature ones. For the third (n-butyl acetate) and fourth (amyl acetate) case studies, the control performance of all three structures is as good as that of the literature structures. For the first case (2-ethylhexyl acrylate) the performance of these structures is acceptable, and fairly close to that of the literature ones. However, for the second (n-butyl acrylate) and fifth (mix of butyl- and amyl acetate) case studies, the control structures S-4 and S-5 fail to at least one of the tested process changes. S-3 shows a good performance for case 2 and acceptable for case 5. It is worth noting that the literature control structures have an excellent performance for all case studies, with some exceptions for case 2 and case 3 to some of the process changes.

While in many cases the performance of the new control structures is good or acceptable, there are also situations when these structures struggle. The main deficiency leading to control difficulties, and in some cases to failure in controlling the process, is the insufficient feedback from inventory measurements. One common situation is when the acid escapes in the overhead of the column. Since the acid is also water-soluble, the aqueous flow from the decanter can contain the acid in large concentration; however, the flow rate does not change significantly so that a control structure measuring the reflux ratio (say, S-4 or S-6) can properly detect the acid and send feedback to the controller so that action can be taken by properly adjusting the fresh reactant flow rate. In the case of a control structure measuring the reflux alone (say, S-5), the situation is even worse, as no feedback at all is received regarding the flow of the aqueous stream.

This study shows, once again, the difficulty of controlling the component inventory in reactive distillation processes. There is no such situation where one control structure fits all reactive distillations, but rather the process for finding a suitable structure (for a particular reaction system) is by investigating the performance of multiple structures and selecting one that fits the purpose. Yet, our expectation is that the process industry community will further study and improve the proposed new control structures.

Declaration of Competing Interest

The authors declare that they have no known competing financial interests or personal relationships that could have appeared to influence the work reported in this paper.

Acknowledgement

The financial support of the European Commission through the European Regional Development Fund and of the Romanian state budget, under grant agreement POC P-37-449 (acronym ASPiRE) is thankfully acknowledged. AAK gratefully acknowledges the Royal Society Wolfson Research Merit Award (No. WM170003). This paper is dedicated to Prof. Andrzej Górak on the occasion of his 70th anniversary, with thanks for the collaboration and valuable discussions along the years.

Supplementary materials

Supplementary material associated with this article can be found, in the online version, at doi:10.1016/j.cep.2021.108672.

References

[1] G.J. Harmsen, Reactive distillation: the front-runner of industrial process intensification. A full review of commercial applications, research, scale-up, design and operation, Chem. Eng. Process. 46 (2007) 774–780.
[2] A.C. Dimian, C.S. Bildea, A.A. Kiss, Integrated design and simulation of chemical processes, Elsevier, Amsterdam, 2014.
[3] W.L. Luyben, B.D. Tyreus, M.L. Luyben, Plantwide Process Control, McGraw Hill Book Co., New York, 1999.
[4] S.G. Huang, C.L. Kuo, S.B. Hung, Y.W. Chen, C.C. Yu, Temperature control of heterogeneous reactive distillation, AIChE J. 50 (2004) 2203–2216.
[5] H. Xu, Q. Ye, H. Zhang, J. Qin, N. Li, Design and control of reactive distillation-recovery distillation flowsheet with a decanter for synthesis of N-propyl propionate, Chem. Eng. Process. 85 (2014) 38–47.
[6] M.D. Moraru, C.S. Bildea, Process for n-butyl acrylate production using reactive distillation: design, control and economic evaluation, Chem. Eng. Res. Des. 125 (2017) 130–145.
[7] M.D. Moraru, C.S. Bildea, Process for 2-ethylhexyl acrylate production using reactive distillation: design, control, and economic evaluation, Ind. Eng. Chem. Res. 57 (2018), 17773-15784.
[8] S.K. Hung, C.S. Lee, H.Y. Lee, C.L. Lee, I.L. Chien, Improved design and control of triacetin reactive distillation process for the utilization of glycerol, Ind. Eng. Chem. Res. 53 (2014) 11989–12002.
[9] C.S. Bildea, A.A. Kiss, Dynamics and control of a biodiesel process by reactive absorption, Chem. Eng. Res. Des. 89 (2011) 187–196.
[10] A.C. Dimian, C.S. Bildea, F. Omota, A.A. Kiss, Innovative process for fatty acid esters by dual reactive distillation, Comput. Chem. Eng. 33 (2009) 743–750.
[11] M.C. Georgiadis, M. Schenk, E.N. Pistikopoulos, R. Gani, The interactions of design control and operability in reactive distillation systems, Comput. Chem. Eng. 26 (2002) 735–746.
[12] S.B. Hung, M.J. Lee, Y.T. Tang, Y.W. Chen, I.K. Lai, W.J. Hung, H.P. Huang, C. C. Yu, Control of Different Reactive Distillation Configurations, AIChE J. 52 (2006) 1423–1440.
[13] W.L. Luyben, C.C. Yu, Reactive Distillation Design and Control, Wiley-AIChE, New York, 2008.
[14] S.S. Mansouri, M. Sales-Cruz, J.K. Huusom, R. Gani, Systematic integrated process design and control of reactive distillation processes involving multi-elements, Chem. Eng. Res. Des. 115 (2016) 348–364.
[15] N. Sharma, K. Singh, Control of reactive distillation column: a review, Int. J. Chem. Reactor Eng. 8 (2010) 1–55.
[16] S. Grüner, K.-.D. Mohl, A. Kienle, E.D. Gilles, G. Fernholz, M. Friedrich, Nonlinear control of a reactive distillation column, Control Eng. Pract. 11 (2003) 915–925.
[17] Z.K. Nagy, R. Klein, A.A. Kiss, R. Findeisen, Advanced control of a reactive distillation column, Comput. Aided Chem. Eng. 24 (2007) 805–810.
[18] D.B. Kaymak, W.L. Luyben, Comparison of two types of two-temperature control structures for reactive distillation columns, Ind. Eng. Chem. Res. 44 (2005) 4625–4640.
[19] M. Al-Arfaj, W.L. Luyben, Comparison of alternative control structures for an ideal two-product reactive distillation column, Ind. Eng. Chem. Res. 39 (2000) 3298–3307.
[20] S. Roat, J. Downs, E. Vogel, J. Doss, Integration of Rigorous Dynamic Modeling and Control System Synthesis For Distillation columns, Chemical Process Control - CPC III, Elsevier, Amsterdam, 1986.
[21] W.J. Hung, I.K. Lai, S.B. Hung, H.P. Huang, M.J. Lee, C.C. Yu, Control of reactive distillation columns for amyl acetate production using dilute acetic acid, J. Chin. Inst. Eng. 29 (2006) 319–335.
[22] S.B. Hung, M.J. Lee, Y.T. Tang, Y.W. Chen, I.K. Lai, W.J. Hung, H.P. Huang, C. C. Yu, Control of different reactive distillation configurations, AIChE J. 52 (2006) 423–1440.
[23] Y.H. Chung, T.H. Peng, H.Y. Lee, C.L. Chen, I.L. Chien, Design and control of reactive distillation system for esterification of levulinic acid and n-butanol, Ind. Eng. Chem. Res. 54 (2015) 3341–3354.
[24] S.J. Wang, C.C. Yu, H.P. Huang, Plant-wide design and control of DMC synthesis process via reactive distillation and thermally coupled extractive distillation, Comput. Chem. Eng. 34 (2010) 361–373.

[25] Q. Pan, L. Gao, J. Li, J. Yan, L. Zhang, J. Liu, M. Sun, L. Sun, Process optimization and plant-wide control for producing 1,3-dioxolane from aqueous formaldehyde solution and ethylene glycol, Sep. Purif. Technol. 236 (2020), 116235.
[26] H.Y. Lee, F.J. Novita, K.C. Weng, Hybrid heat-integrated design and control for a diphenyl carbonate reactive distillation process, Chem. Eng. Process. 162 (2021), 108344.
[27] K.-.L. Zeng, C.-.L. Kuo, I.-.L. Chien, Design and control of butyl acrylate reactive distillation column system, Chem. Eng. Sci. 61 (2006) 4417–4431.
[28] M.D. Moraru, E. Zaharia, C.S. Bildea, Novel control structures for heterogeneous reactive distillation, Chem. Eng. Trans. 69 (2018) 535–540.
[29] M.D. Moraru, C.S. Bildea, One-point temperature control of reactive distillation: a thermodynamics-based assessment, Comput. Aided Chem. Eng. 46 (2019) 1201–1206.
[30] M. Al-Arfaj, W.L. Luyben, Control of ethylene glycol reactive distillation column, AIChE J. 48 (2002) 905–908.
[31] A. Niesbach, H. Kuhlmann, T. Keller, P. Lutze, A. Gorak, Optimisation of industrial-scale n-butyl acrylate production using reactive distillation, Chem. Eng. Sci. 100 (2013) 360–372.
[32] H.Y. Lee, L.T. Yen, I.L. Chien, H.P. Huang, Reactive distillation for esterification of an alcohol mixture containing n-butanol and n-amyl alcohol, Industrial & Engineering Chemistry Research 48 (2009) 7186–7204.
[33] J. Gangadwala, S. Mankar, S. Mahajani, A. Kienle, E. Stein, Esterification of acetic acid with butanol in the presence of ion-exchange resins as catalysts, Ind. Eng. Chem. Res. 42 (10) (2003) 2146–2155.